Planetary and Space Science 182 (2020) 104796

Contents lists available at ScienceDirect

Planetary and Space Science

journal homepage: www.elsevier.com/locate/pss

Rapid falling of an orbiting moon to its parent planet due to tidal-seismic resonance

Yuan Tian *, Yingcai Zheng

Department of Earth and Atmospheric Sciences, University of Houston, Houston, TX, USA

ARTICLE INFO

Keywords:
Resonance
Tidal force
Normal mode
Orbital evolution
Tidal-seismic resonance

ABSTRACT

Tidal forces play an important role in the evolution of the planet-moon systems. The tidal force of a moon can excite seismic waves in the planet it is orbiting. A tidal-seismic resonance is expected when a tidal force frequency matches a free-oscillation frequency of the planet. Here we show that when the moon is close to the planet, the tidal-seismic resonance can cause large-amplitude seismic waves, which can change the shape of the planet and in turn, exert a negative torque on the moon causing it to fall rapidly toward the planet. We postulate that the tidal-seismic resonance may be an important mechanism, which can accelerate the planet accretion process. On the other hand, the tidal-seismic resonance effect can also be used to interrogate the planet's interior by long term tracking of the orbital change of the moon.

1. Introduction

Darwin (1898) first proposed the idea of a gravity-seismic coupled resonance of a fluid planet to explain the Moon formation. He argued that the violent vibration of the planet at resonance "… *shook the planet to pieces, detaching huge fragments which ultimately were consolidated into the Moon.*" While Darwin's idea of moon formation theory has been largely discarded, very little work has been done to investigate possible consequences of the tidal-seismic resonance for a planet-moon system, in particular for a solid planet.

Tidal force frequencies are usually out of the range of planet free oscillation (or normal mode) frequencies. Even the tidal force of the very fast orbiting Phobos around Mars does not produce a significant effect on the Martian free oscillation in the current orbital configuration (Lognonné et al., 2000).

However, in some cases, tidal force frequencies can intrude into the frequency range of the planet's normal modes. For example, the tidal force on a rapidly rotating planet can excite the normal modes of the planet (Braviner and Ogilvie, 2014a, b; Barker et al., 2016). Interaction between Saturn's ring and Saturn can excite the acoustic free oscillation of Saturn (Marley, 1991, 2014; Marley and Porco, 1993). Fuller (2014) used the tidal force to detect the acoustic free oscillation frequencies by observing density waves in the Saturn ring. Furthermore, Fuller et al. (2016) also studied the resonance between tidal force and the acoustic free oscillation of gas giants (e.g., Saturn and Jupiter) which could change the migration of the moons.

Our goal here is to do a theoretical and numerical analysis to investigate some first-order effects of tidal-seismic resonance for a solid planet.

2. Material and methods

2.1. Model setup

In our analysis, it is better to make some simplifications and approximations to focus on the tidal-seismic resonance effect. We consider a planet-moon system as a binary rotating system in an inertial reference frame. We assume the moon is a point mass and we do not consider potential fragmentation of the moon at the Roche limit (Aggarwal and Oberbeck, 1974; Asphaug and Benz, 1994; Black and Mittal, 2015). The modeled planet does not spin with respect to the reference frame. We assume that the moon's orbit is circular along the planet's equatorial plane. The orbiting period of the moon can be computed using Kepler's laws. We compute the moon's tidal force for every point inside the planet by subtracting the centrifugal force from the gravitational attraction force for the moon.

We consider two planetary models: model-1 with no topography, and model-2 with topography. In model-1, the planet is a homogeneous, elastic, and spherical solid with no topography. We set the compressional wave velocity in the solid as $v_p = 3$ km/s and the shear wave velocity $v_s = 1.2$ km/s. We set the radius of the planet as 2000 km. We use the mass-

* Corresponding author.
E-mail address: ytian9@cenral.uh.edu (Y. Tian).

https://doi.org/10.1016/j.pss.2019.104796
Received 18 January 2019; Received in revised form 7 November 2019; Accepted 12 November 2019
Available online 19 November 2019

radius relation (Chen and Kipping, 2017) to set the planet density as $\rho = 2840\ kg/m^3$. For this planet, the shear modulus is low in our model which could represent an icy body known to have low shear modulus (e.g., Nimmo et al., 2007) or a planet with a liquid core which can effectively lower the entire shear modulus. The mass of the moon is taken as, 10^{16} kg (as a reference, this is similar to the mass of an object like Phobos), which is about 10^{-7} times of the mass of the planet. We also consider the effect of Q, which captures the dissipation effect of the planet. Previous researchers showed that Q could cause a tidal phase lag and was important in calculating the orbital decay of the moon (Zharkov and Gudkova, 1997; Bills et al., 2005; Nimmo and Faul, 2013; Zheng et al., 2015). We also consider a second planetary model of the same material (model-2), but with a randomly generated topography to study how planet topography can also play a role in the tidal-seismic resonance.

2.2. Method

To see when the tidal-seismic resonance can occur, we can compute the planet's normal-mode frequencies (see Appendix-A) and tidal force frequencies (Appendix-B). Because the moon orbits around the planet periodically, the tidal force is periodic at any point in the planet. If the orbital frequency is designated as ω_0, we also expect to see higher-order harmonics such as $n\omega_0$ where n = 2, 3, 4, …. The tidal-seismic resonance occurs when a tidal force frequency is the same as a normal-mode frequency (Fig. 1). The tidal force preferentially excites the fundamental spheroidal normal mode, ${}_0S_n$, where n is the degree in the surface spherical harmonic function.

The orbiting moon exerts a cyclic tidal force for every point in the planet. Therefore, this tidal force can cause seismic displacement in the planet, which leads to the deformation of the planet. The change of the figure of the planet can alter the planet's gravitational field to exert a net torque on the moon. To compute this torque, we need to compute the tidal force induced seismic wavefield. We used the boundary element integral equation approach (Zheng et al., 2016) (also see Appendix C). The advantage of this computational method is that it is directly implemented in the frequency domain and can model long-term seismic field evolution (i.e., can avoid numerical dispersion in many time-domain methods) and can also handle planet topography. To focus on the tidal-seismic resonance effect, we did not consider the effect of gravity on the propagation of the seismic wave (Dahlen and Tromp, 1998) in our calculation. Once we obtain the seismic wavefield, we can compute the time-dependent torque on the moon and the orbital decay rate of the moon (See Appendix D). As an important verification of our numerical approaches, we compare our numerical torque results against the analytical torque calculation for model-1. We found that the two results are in excellent agreement (See Appendix E, Figure A2).

3. Results

3.1. Tidal-seismic resonance at low orbits

At low orbits, it can be seen that the orbital decay rate overall is increasing as the moon is approaching the planet and the tidal seismic effect punctuates/accelerates this trend locally at several distinct orbital radii ("peaks" in Fig. 2). The locations of the "peaks" correspond to special orbital radii at which strong torque has been exerted on the orbiting moon due to the tidal-seismic resonance. Because of their special importance, we call these orbital radii r_n^*, where $n = 2, 3\ldots$. At r_n^*, the planet ${}_0S_n$ normal mode frequency is exactly n times of the moon's orbital frequency. In these cases, both the tidal force and the ${}_0S_n$ mode have degree-n spatial patterns within the planet. Therefore, it is a simultaneous coupling for both the temporary and spatial frequencies (i.e., degree-n) at r_n^*, which can cause a very strong excitation of seismic displacement inside the planet (Fig. 2).

We then compute orbital decay rates for several different Q values (see Appendix D for details). In general (i.e., no tidal-seismic resonance), the decay rate is small if Q is large because the tidal phase lag proportional to $1/Q$ is small (see Bills et al., 2005). However, at r_n^* where the tidal-seismic resonance happens, the opposite is true because a large Q yields a large induced seismic displacement, which gives a large torque causing a large decay rate (Fig. 2). Among all r_n^*'s, the r_2^* is special. At r_2^* where the degree-2 normal mode (i.e., the gravest "football-shaped" mode) is excited by the tidal force, the orbital decay rate is computed and found to be on the order of ~1–10 cm/s for different Q values (Fig. 2) for this particular planet/moon model (i.e., model-1) considered here. At the tidal-seismic resonance orbit, the orbital decay rate is 2 orders of magnitude more than that for a neighboring orbit that has no resonance.

We note that the exact numerical value for orbit decay may vary from model to model. However, the tidal-seismic resonance can significantly accelerate the orbital decay ("peaks" in Fig. 2 compared to the smooth background trend). The greater the Q value is, the sharper the peaks are. To verify whether these peaks are indeed caused by the tidal-seismic resonance effect, we analytically calculated the normal mode ${}_0S_n$ frequencies of the planet (See Appendix A). We then calculated the corresponding r_n^* whose orbital frequency is $1/n$ times of the ${}_0S_n$ frequency. We

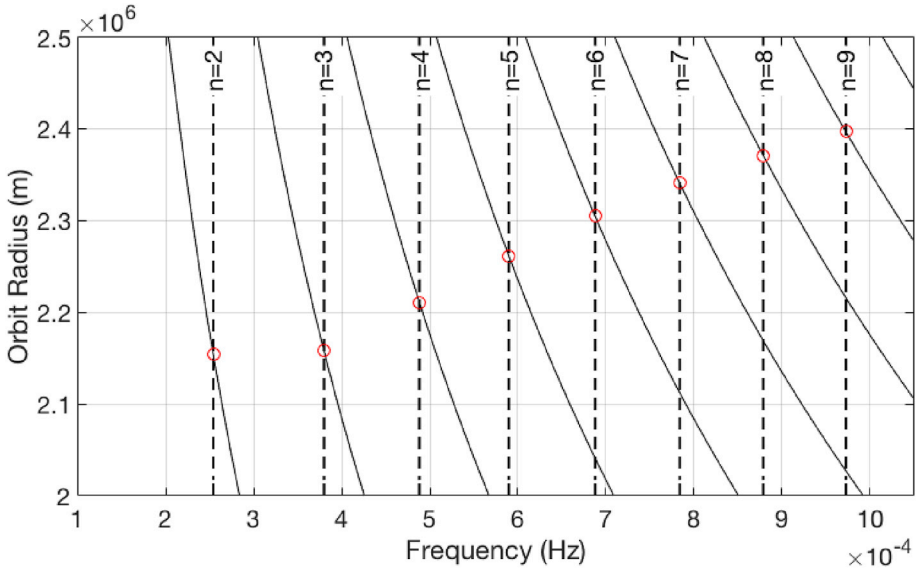

Fig. 1. Tidal force and planet normal mode frequencies for model-1. The solid lines are tidal force frequencies calculated for a point on the planet equator. The vertical dashed lines are the planet free-oscillation frequencies for the spheroidal ${}_0S_n$ normal modes (n = 2, 3, 4, …). The tidal-seismic resonance occurs when tidal force frequencies intersect the planet free oscillation frequencies at the red circles. (For interpretation of the references to colour in this figure legend, the reader is referred to the Web version of this article.)

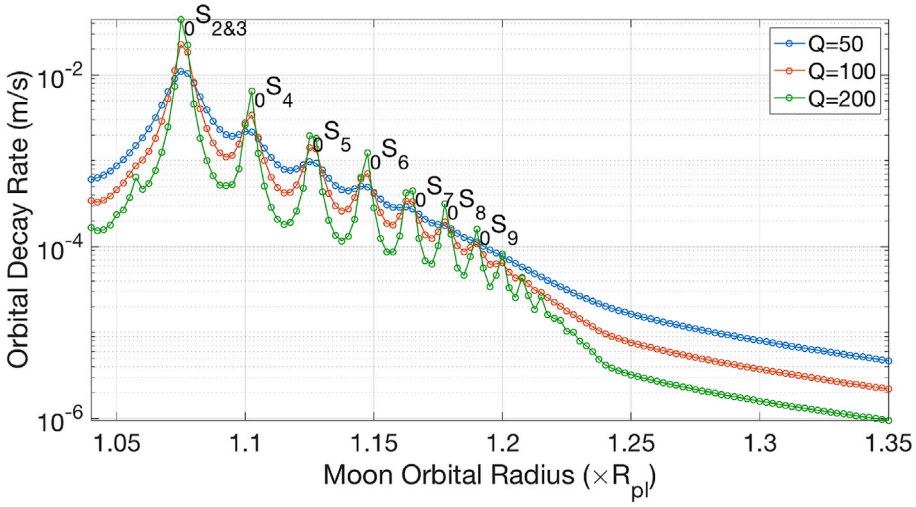

Fig. 2. Calculated moon orbital decay rates at different orbital radii and for different Q values for model-1. The horizontal axis is the radius of the moon orbit. The radius of the planet R_{pl} is 2×10^6m. We also label the excited normal modes, S_n, $n \geq 2$, expected to be seen for the tidal-seismic resonance.

found that the calculated r_n^* based on the ${}_0S_n$ frequency corresponds to the "peaks" of the moon orbital decay rate (Fig. 2). In conclusion, the rapid falling of the moon is caused by the tidally excited seismic normal modes of the planet. When the moon's orbit radius is large (e.g., $>2.5\times 10^6$m or $>1.25R_{pl}$), the tidal-seismic resonance effect is not pronounced. In this case, a smaller Q value gives a larger orbital decay rate which is consistent with the tidal drag due to the anelasticity effect (Bills et al., 2005).

3.2. Topography induced tidal-seismic resonance

At higher orbits (orbital radius greater than $2.5\times 10^6 m$ or $1.25\ R_{pl}$ in this case), the tidal seismic resonance can occur when $m\omega_0$ matches the S_n frequency, where both m and n are integers and typically $m > n$.

In principle, a degree-m tidal force field cannot excite degree-n normal mode for a purely spherical and homogeneous planet (i.e., model-1) because these two fields are orthogonal to each other in space. However, if the planet is not spherical (i.e., model-2), the tidal-seismic resonance can still exist because topography could couple modes of different spatial degrees. Our purpose here is to investigate the topography-induced tidal-seismic effect.

For model-2, we generated the surface topography for the planet using spherical harmonics up to and including order 6 (Fig. 3). Specifically, the topography, h, is generated by the summation of spherical harmonics, $h(\theta,\varphi) = \sum_{l=0}^{6}\sum_{m=-l}^{l} c_{lm} Y_l^m(\theta,\varphi)$, where h is the height of the topography from the reference sphere, θ and φ are the angular positions on the surface, and Y_l^m represents the fully normalized spherical harmonics. We generate random numbers for the coefficients, c_{lm} to construct the topography for model-2. We use the same numerical procedure laid out in Section 3.1 to compute the seismic wavefield for model-2, along with the torque on the moon and the orbital decay rate of the moon. To see the topography effect on the tidal seismic resonance, we take the derivative of the orbital decay rate with respect to the orbital radius and several localized changes at some radii show up (Fig. 4a). These changes are due to topography induced tidal-seismic resonance. To validate this claim, we run our seismic wavefield modeling using our two models (model-1 and model-2) and obtain histories of orbital decay rates for both models. We then calculate the derivative of the orbital decay rate with respect to the orbital radius for the two models (Fig. 4 a &b). We can see localized changes for the topography model, model-2 (Fig. 4a). In contrast, we see a smooth curve (no localized changes) for the orbital decay rate derivative using model-1 with no topography (Fig. 4b). Hence,

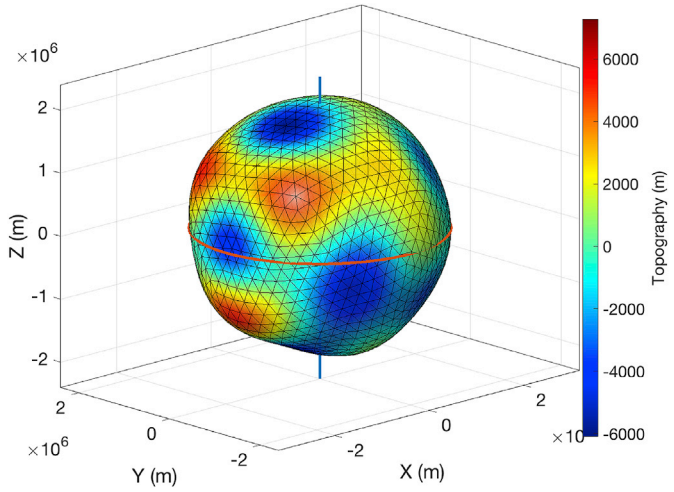

Fig. 3. A model with topography (model-2) for the planet. We have exaggerated the plotting of the topography by 20 times. Colors indicate topography relative to the mean radius of the planet with size given in meters. The thick red line is the equator. The blue vertical thick line is the axis through the poles. (For interpretation of the references to colour in this figure legend, the reader is referred to the Web version of this article.)

topography can indeed induce tidal-seismic resonance at higher orbits.

4. Discussions

Tidal forces play an important role in the orbital evolution of the Martian moon, Phobos (Black and Mittal, 2015; Hesselbrock and Minton, 2017) because Phobos is below the synchronous orbit. Phobos is spiraling towards Mars due to the tidal torque. Will our proposed tidal-seismic resonance effect play a role in this system? Presently, Phobos' orbit radius is about 2.77 times the Mars radius (Rm), which is too far to induce a significant tidal-seismic resonance. However, when Phobos' orbit decays to about $1.97\ \times Rm$, the topography induced tidal-seismic resonance will occur, provided Phobos is strong enough and not fragmented by Mars gravity field at the Roche limit. The strength of Phobos depends on the internal friction angle of the material in Phobos. A Roche limit of $1.97\ \times$ Rm corresponds to an internal friction angle of 40° (Holsapple and Michel, 2006). If the angle is larger than 40° (Holsapple and Michel, 2006) (i.e., a stronger Phobos), the tidal seismic resonance can occur

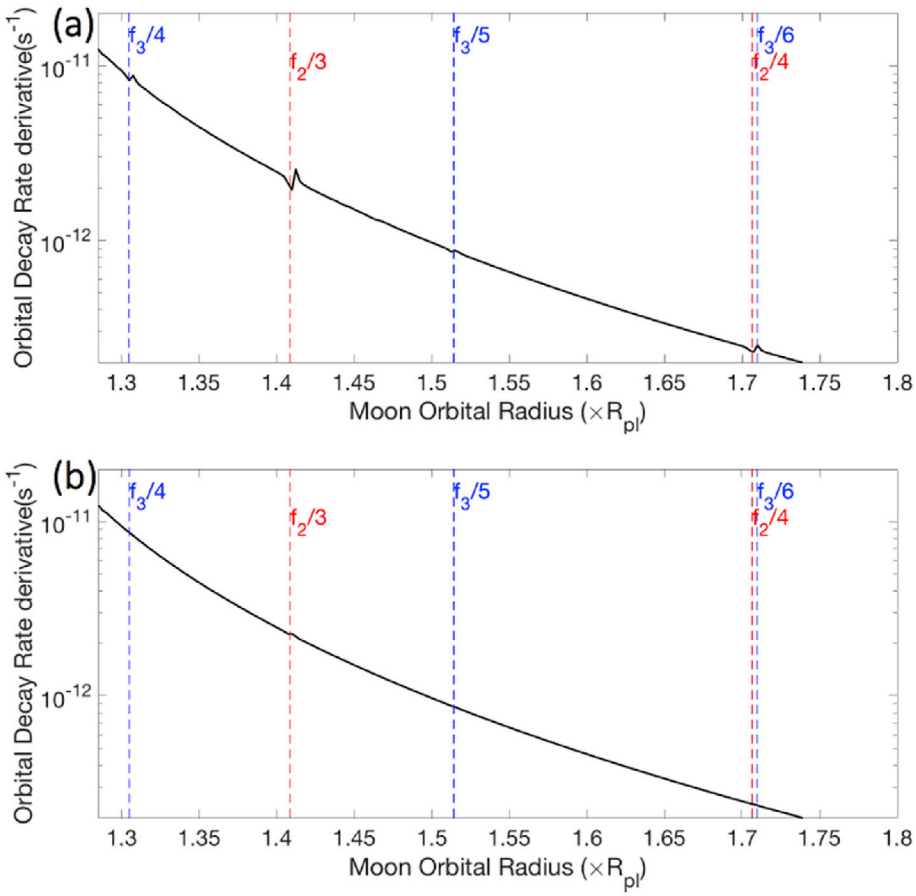

Fig. 4. The derivative of the orbital decay rate with respect to the orbital radius for (a) model-2 with topography and (b) model-1 with no topography. Here, f_n is the frequency of the normal mode S_n. A dashed line shows the orbit whose orbital frequency is f_n/m, where n and m are integers and labeled accordingly next to the dashed line. The radius of the planet R_{pl} is 2×10^6m.

before Phobos reaches the Roche limit. When Phobos' orbit is at $1.97 \times Rm$, we estimate the orbital decay rate to be about $10^{-10} m/s$ based on the present-day Martian topography using an approximate homogenous Mars model (P-wave velocity $v_p = 7.4 km/s$, S-wave velocity $v_s = 3.6 km/s$, density $\rho = 4000 kg/m^3$ to match a ${}_0S_2$ period of about 2300 s (Zheng et al., 2015)). This rate is about 8% of the current orbital decay rate of Phobos, which is approximately $1.28 \times 10^{-9} m/s$ (Bills et al., 2005). As Phobos continues falling towards Mars, the effect of tidal-seismic resonance will be more and more powerful in pulling Phobos towards Mars. Because of the tidal-seismic resonance, we note that Phobos cannot stay at low orbits for a long time even if it is below the Roche limit and not fragmented.

5. Conclusions

The tidal-seismic resonance effect can be important in understanding planet-moon evolution if the moon is below the synchronous orbit. The tidal seismic resonance can result in a large negative torque on the orbiting moon, which can increase the orbital decay rate of the moon toward the planet it is orbiting by one order of magnitude. It is also conceivable that the tidal-seismic resonance may also significantly accelerate the planetary accretion and formation process. The tidal-seismic phenomenon may also provide us with a potential method for interrogating the structure and compositional information of a planet without having to land an instrument on its surface. By precisely measuring the orbital decay rate as a function of radii, we can infer the normal mode frequencies of the planet, which can convey a wealth of information about the planet's interior.

Declarations of interest

None.

Declaration of competing interest

None.

Acknowledgments

We thank the editor and the two anonymous reviewers for insightful recommendations. We are also very grateful to Paige Given who helped proofread the manuscript for English. We thank Prof. Francis Nimmo for pointing out the work by G.H. Darwin to us. We thank Dr. Hao Hu for offering help in the analytical torque calculation. The work is partially supported by the U.S. National Science Foundation grants EAR-1621878 and EAR-1833058. We thank UHXfrac for providing computing resources.

Appendix A. Supplementary data

Supplementary data to this article can be found online at https://doi.org/10.1016/j.pss.2019.104796.
The Mathematica script for computing the tidal Love number can be accessed freely at https://github.com/ytian159/Love-number.

Appendices.

A. Calculation of the normal-mode frequencies of a homogenous solid planet

A planet can resonate as a whole at certain discrete frequencies and spatial patterns. These vibrational modes are called seismic normal modes (p. 337, Aki and Richards, 2002). There are two types of modes: spheroidal modes associated with volumetric changes, and toroidal modes not associated with volumetric changes. Thus, only spheroidal modes contribute to the tidal torque for a homogenous, spherical, solid planet.

By applying a free surface condition, we can analytically solve for the frequencies of spheroidal modes for a spherical and elastic uniform body (see p. 364, Ben-Menahem and Singh, 1981).

$$\frac{2(1-l+k_\alpha a S_\alpha)}{\left[-2+2l^2-(k_\beta a)^2+2k_\beta a S_\beta\right]}-\frac{\left[2l(l-1)-(k_\alpha a)^2\tau^2+4k_\alpha a S_\alpha\right]}{2l(l+1)[(l-1)-k_\beta a S_\beta]}=0, \tag{A.1}$$

where a is the planet radius, $S_\alpha = j_{l+1}(k_\alpha a)/j_l(k_\alpha a)$, $S_\beta = j_{l+1}(k_\beta a)/j_l(k_\beta a)$, j_l is the spherical Bessel function of the angular order l ($l = 0,1,2\ldots$), k_α and k_β are the P and S wavenumbers respectively, and $\tau = k_\beta/k_\alpha$. The temporary frequencies are included in wavenumbers as, $k_\alpha = \frac{\omega}{v_p}, k_\beta = \frac{\omega}{v_s}$. As an example, we can solve equation (A.1) to get the frequencies of spheroidal modes (Fig. A1 with parameters, $a = 2000km$, $v_p = 3km/s$, $v_s = 1.2km/s$.

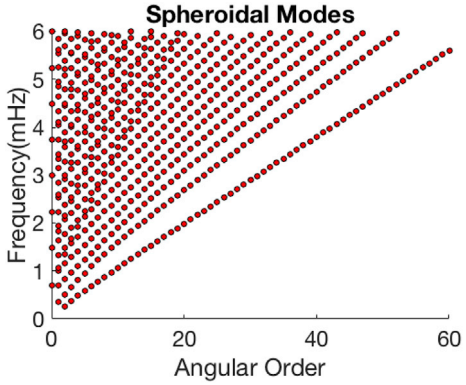

Fig. A1. The normal-mode frequencies of the planetary model, model-1. This plot shows the frequencies of the spheroidal mode frequencies at different angular orders.

B. Calculation of the tidal force in the planet due to the orbiting moon

The tidal force of the orbiting moon is following Newton's law of universal gravitation. We can obtain the formula of the tidal force acceleration, **g**, at **x'**:

$$\mathbf{g}(\mathbf{x}',t)=\frac{Gm_m}{|\mathbf{x}_m(t)-\mathbf{x}'|^3}[\mathbf{x}_m(t)-\mathbf{x}']+\mathbf{f}_{cf}(\mathbf{x}',t), \tag{B.1}$$

where $\mathbf{x}_m(t)$ is the position of the moon at time t on a circular orbit with a constant angular speed, ω_0. G is the universal gravitational constant. m_m is the mass of the moon. $\mathbf{f}_{cf}(\mathbf{x}',t)$ is the centrifugal force at **x'**. We can use this formula to calculate the excitation of the seismic field for our seismic wavefield modeling later (Appendix C).

Although the moon's orbital frequency is ω_0, it can also generate other higher harmonic frequencies. To see this, we can analyze the first term in (B.1) by looking at its gravitational potential (Taylor and Margot, 2010)

$$V(\mathbf{x},t)=-\frac{Gm_m}{|\mathbf{x}_m(t)-\mathbf{x}|}=-\sum_{n=1}^{\infty}\frac{Gm_m|\mathbf{x}|^n}{r_m^{n+1}}P_n[\cos\psi(t)], \tag{B.2}$$

where P_n is n-th order Legendre polynomial, $\psi(t)$ is the angle between vectors **x** and $\mathbf{x}_m(t)$, and r_m is the radius of the moon's circular orbit along the planet's equatorial plane. For a point **x** in the planet, the gravity potential is changing with time due to the term in the Legendre polynomial, $P_n[\cos\psi(t)]$. If the orbit frequency is ω_0, $P_n[\cos\psi(t)]$ has the term $\cos(n\omega_0 t)$, whose frequency is $n\omega_0$ (n = 0, 1, 2, …). Therefore, the tidal force frequencies of the moon are discrete and have higher order harmonics. We note that the centrifugal force can cancel the term $n = 1$ of the gravitational potential V. Therefore, n should start from 2, and the tidal potential is:

$$V_{tide}(\mathbf{x},t)=-\sum_{n=2}^{\infty}\frac{Gm_m|\mathbf{x}|^n}{r_m^{n+1}}P_n[\cos\psi(t)] \tag{B.3}$$

In the examples in this paper, we truncate the angular order to $n = 16$ in equation (B.3) for our numerical simulation. We have tested that any higher order tidal force term has no significant contribution in the sum (equation (B.3)); thus, we ignored the higher order polynomials. We consider the case that the mass of the moon is much smaller than the planet; therefore, the center of the planet is almost the same as the center of mass of the two-body system.

C. Modeling seismic wavefield in the planet with topography using the boundary element method (BEM)

We used the Boundary Element Method (BEM) (Zheng et al., 2016) to numerically model the seismic field of the planet excited by the tidal force, which follows Eqn C.1:

$$-\rho\nabla V_{tide} + \nabla\cdot\sigma = \rho\ddot{\boldsymbol{u}}, \tag{C.1}$$

where σ is the elastic stress tensor, V_{tide} is the tidal potential from (B.3), $\boldsymbol{u}$ is the seismic displacement.

In our seismic modeling, the planet can have an arbitrary surface topography. The BEM method is a frequency domain method, which can reduce the computational cost of this study. The BEM method computes the full seismic wavefield, including all possible normal mode coupling between spheroid and toroidal modes. BEM first solves the wavefield on the planetary surface/boundary. Once the boundary field is known, we can compute the wavefield at any point inside the planet using the representation theorem (p. 28, Aki and Richards, 2002). The boundary integral equation governs the seismic field, $\mathbf{u}$:

$$\frac{1}{2}u_q(\mathbf{x},\omega) = u_{0q}(\mathbf{x},\omega) - \int_S u_i(\mathbf{x}')C_{ijkl}(\mathbf{x}')G_{kq,l}(\mathbf{x}',\mathbf{x},\omega)n_j d\mathbf{x}'^2; \quad \mathbf{x},\mathbf{x}' \in S. \tag{C.2}$$

In this equation, S is the surface of the planet including topography; n_j is the outward surface normal along j-th direction; $C_{ijkl}(\mathbf{x}')$ is the elastic constant matrix of the planet model at $\mathbf{x}'$. Here, we assume the planet is isotropic, so there are only two independent Lame parameters in the matrix. $G_{kq,l}(\mathbf{x}',\mathbf{x},\omega)$ is the elastic Green's function derivative with respect to $\mathbf{x}'$ along the l-th direction in the frequency domain. All subscripts (q, i, j, k, l) in equation (4) take a value of 1, 2, or 3 to indicate the component of the vector/tensor field. The medium Q factors for P and S waves is in the Green's function.

The incident field, $u_{0q}(\mathbf{x},\omega)$, excited by the tidal force (see equation (B.1)) along the q-th direction in the frequency domain can be computed as:

$$u_{0q}(\mathbf{x},\omega) = \int \rho(\mathbf{x}')g_i(\mathbf{x}',\omega)G_{iq}(\mathbf{x},\mathbf{x}',\omega)dx'^3, \tag{C.3}$$

where $\mathbf{x}$ and $\mathbf{x}'$ are points in the planet. $G_{iq}(\mathbf{x},\mathbf{x}',\omega)$ is the Green's function in a homogeneous unbounded elastic medium. $g_i(\mathbf{x}',\omega)$ is the tidal force of the moon at $\mathbf{x}'$ along the i-th direction in the frequency domain. The value of $g_i(\mathbf{x}',\omega)$ at each frequency is the Fourier coefficient of equation (B.2):

$$\mathbf{g}(\mathbf{x}',\omega) = \frac{1}{T}\int_0^T \mathbf{g}(\mathbf{x}',t)e^{i\omega t}dt, \tag{C.4}$$

where T is the orbital period. The frequency ω takes discrete values ($n\omega_0$) as showed in equation (C.4), where $n = 1, 2, 3\ldots$.

To solve equation (C.2), we partition the planet surface into small triangles. Each triangle is called a boundary element. We assume the seismic wavefield $\mathbf{u}(\mathbf{x},\omega)$ on each surface element is constant. We can then discretize equation (C.2) and get a system of coupled linear equations:

$$\left(\frac{1}{2}I + A\right)[u] = [u_0], \tag{C.5}$$

where A is a matrix representing wavefield interaction between the surface elements. Matrix A depends on the geometry of the surface and the medium elastic properties; $[u]$ is a vector containing the 3-component surface displacements on all the elements. I is an identity matrix. $[u_0]$ is a vector containing the incident field on all surface elements, excited by the tidal force and calculated using equations (C.3) and (C.4). In the BEM method, we invert for the surface displacement [u] on each element by solving the linear algebraic equation (C.5). Now, we have obtained seismic displacement $\mathbf{u}(\mathbf{x},\omega)$ on each surface element. By the representation theorem (p.28, Aki and Richards, 2002), we can compute the displacement field at any point within the planet.

Because the tidal force is discrete in frequency, we only need to solve equation (C.5) at these discrete frequencies. Once we get $\mathbf{u}(\mathbf{x},\omega)$ at frequency $n\omega_0$, we can use Fourier series to get the time-domain field, $\mathbf{u}(\mathbf{x},t)$:

$$\mathbf{u}(\mathbf{x},t) = \sum_{n=1}^{N} 2\mathrm{Re}[\mathbf{u}(\mathbf{x},n\omega_0)e^{in\omega_0 t}], \tag{C.6}$$

where Re takes the real part of a complex number, N is the truncation angular order and we set $N = 16$. Because $\mathbf{u}(\mathbf{x},t)$ is linearly proportional to $[u_0]$ which is linearly proportional to the mass of the moon, $\mathbf{u}(\mathbf{x},t)$ is also proportional to the mass of the moon.

D. Calculation of the tidal-seismic torque and the orbital decay rate

Once we have obtained the seismic displacement, $\mathbf{u}(\mathbf{x},t)$, we can compute the time-t dependent torque on the moon due to the seismic wavefield in the planet:

$$\boldsymbol{M}(t) = \iint \rho \boldsymbol{r}_m(t) \times G m_m \frac{\mathbf{x} - \mathbf{x}_m(t)}{|\mathbf{x} - \mathbf{x}_m(t)|^3} [\mathbf{u}(\mathbf{x}, \mathrm{t}) \cdot \mathbf{e}_r] d\mathbf{x}^2, \tag{D.1}$$

where, $\mathbf{x}_m$ is the location of the orbiting moon; ρ is the density of the planet; and $\boldsymbol{e}_r$ is the surface normal at $\mathbf{x}$.

We can derive the orbital decay rate of the moon ($\dot{r}_m(t) = dr_m(t)/dt$) by using the Newton's second law:

$$|\dot{r}_m(t)| = \frac{2|\overline{\boldsymbol{M}(t)}|}{m_m} \sqrt{\frac{r_m(t)}{G m_{pl}}}, \tag{D.2}$$

where $\overline{\boldsymbol{M}(t)}$ is the average torque on the moon in one orbital period, G is the universal gravitational constant, m_m is the mass of the moon, and m_{pl} is the mass of the planet.

We have shown that both $\mathbf{g}(\mathbf{x}, t)$ and $\mathbf{u}(\mathbf{x}, t)$ are proportional to the mass of the moon in Appendix B and Appendix C. In equation (D.2), the orbital decay rate is divided by the mass of the moon m_m. Thus, the orbital decay rate is proportional to the mass of the moon. If the mass of the moon changes, the orbital decay rate will change accordingly.

E. Tidal Love number h_2 for a compressible planet

We used BEM to compute the tidal deformation and the seismic wavefield in the planet and the resultant tidal torque. The purpose of this appendix is to show that our BEM (Appendix C) and the torque calculation (Appendix D) are correct by comparing the results to known analytical expressions under the validity regime of such expressions.

Definition of the tidal Love number

The tidal Love number h_2 is defined as a ratio of the radial displacement on the solid planet surface due to the moon's degree-2 tidal potential and the tidal height raised on a hypothetical fluid planet due to the same degree-2 tidal potential. Another tidal Love number is k_2. Assuming the moon is orbiting the planet on the planet's equatorial plane, the tidal Love number is defined as, $h_2 = u_r/(V_{tide}/|\mathbf{g}_0(a)|$, where u_r is the radial displacement on the equator caused by V_{tide} which is the degree-2 tidal potential, and $\mathbf{g}_0(a)$ is the gravitational acceleration on the planet surface. Both V_{tide} and $\mathbf{g}_0(a)$ are known. Computing h_2 is equivalent to computing u_r.

Analytical solution for tidal u_r under self-gravitation

The tidal force can deform the planet and the displacement can be obtained by solving the following Eqn E.1(e.g., Love, 1911) which do not have the seismic wave induced particle acceleration term $\ddot{\boldsymbol{u}}$:

$$-\rho \nabla V_{tide} + \nabla \cdot \sigma - \nabla(\rho \mathbf{u} \cdot \mathbf{g}_0) + \rho \nabla \mathrm{K} + \rho \mathbf{g}_0 \nabla \cdot \mathbf{u} = 0,$$

$$\nabla^2 K - 4\pi G \rho \nabla \cdot \mathbf{u} = 0 \tag{E.1}$$

where is the displacement within the planet caused by the tidal force. Here, V_{tide} is the tidal potential of degree-2 that causes the deformation, σ is the elastic stress tensor, K is the gravitational potential caused by the density perturbation due to seismic waves, and $\mathbf{g}_0$ is the vector gravitational acceleration of the planet. The above equations are solved using zero-traction boundary condition on the planet surface. The terms involving $\mathbf{g}_0$ and K are due to the planet self-gravitation. These terms can be ignored if the tidal force frequency is high.

The tidal Love number, h_2, for a homogeneous planet under degree-2 tidal potential can be found to be Eqn E.2(Love, 1911; Murray and Dermott, 1999),

$$h_2 = \frac{5}{2}\left(1 + \frac{19\mu}{2\rho g_0 a}\right)^{-1}, \tag{E.2}$$

where μ is the shear modulus of the planet, ρ the density of the planet, g_0 is the planet's gravity on its surface, and a is the planet's radius. Using the parameters in this paper, we obtain $h_2 = 0.47$, under the assumptions that 1) the planet is incompressible, i.e., $\mu/\lambda \to 0$, where μ and λ are the two Lamé constants (see Love, 1911, p109); and 2) the planet has self-gravitation. The tidal torque Γ can be computed as (p.164 of Murray and Dermott, 1999)

$$\Gamma = \frac{9}{10} h_2 \frac{G m_m^2}{r_p} \left(\frac{a}{r_p}\right)^5 \sin(2\varepsilon),\ 2\varepsilon = Q^{-1}, \tag{E.3}$$

where m is the mass of the moon, r_p is the moon's orbit radius, and Q is the shear quality factor.

Analytical solution for tidal u_r without self-gravitational effect

However, in our paper we emphasized the effect of resonance. We ignored self-gravitation effect on the propagation of seismic waves. To get the new h_2 value, we need to solve for the following equation

$$-\rho \nabla V_{tide} + \nabla \cdot \sigma = 0, \tag{E.4}$$

with the traction-free boundary conditions on the planet surface. The forcing potential V_{tide} is degree-2.

We then apply the definition of the tidal Love number and numerically solve equation (E.4) and obtain $h = h^* = 0.5877$ for the model and orbital parameters we considered in the main text. A computer script (Mathematica®) is provided to compute the tidal Love number h_2. Our numerical torque calculation, based on the boundary element modeling (equations C.6 and D.1), agrees well with the analytical calculation (E.2) based on h_2^* Fig. A2. Discrepancies at low orbit heights are expected (Fig. A2), as the tidal potential is no longer degree-2. We also note that the torque is inversely proportional to Q. As expected, we see a factor of 4 for the numerical torque values for two different Q values, $Q = 50$ and $Q = 200$, at the same orbital radius.

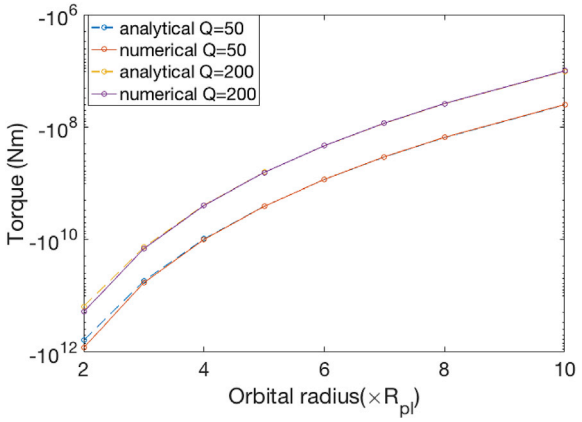

Fig. A2. Comparison of the analytical torque and numerical torque (based on our boundary element modeling, see equation (D.1)) for different orbital radii and Q values. The analytical torque is computed using equation (E.3) with $h_2 = 0.5877$. R_{pl} is the planet's radius.

References

Aggarwal, H.R., Oberbeck, V.R., 1974. Roche limit OF a solid body. Astrophys. J. 191, 577–588.

Aki, K., Richards, P.G., 2002. Quantitative Seismology.

Asphaug, E., Benz, W., 1994. Density of comet shoemaker-levy-9 deduced by modeling breakup of the parent rubble-pile. Nature 370, 120–124.

Barker, A.J., Braviner, H.J., Ogilvie, G.I., 2016. Non-linear tides in a homogeneous rotating planet or star: global modes and elliptical instability. Mon. Not. R. Astron. Soc. 459, 924–938.

Ben-Menahem, A., Singh, S.J., 1981. Seismic Waves and Sources. Springer-Verlag New York Inc.

Bills, B.G., Neumann, G.A., Smith, D.E., Zuber, M.T., 2005. Improved estimate of tidal dissipation within Mars from MOLA observations of the shadow of Phobos. J. Geo. Res. Planets 110.

Black, B.A., Mittal, T., 2015. The demise of Phobos and development of a Martian ring system. Nat. Geosci. 8, 913–U936.

Braviner, H.J., Ogilvie, G.I., 2014a. Tidal interactions of a Maclaurin spheroid–I. Properties of free oscillation modes. Mon. Not. R. Astron. Soc. 441, 2321–2345.

Braviner, H.J., Ogilvie, G.I., 2014b. Tidal interactions of a Maclaurin spheroid–II. Resonant excitation of modes by a close, misaligned orbit. Mon. Not. R. Astron. Soc. 447, 1141–1153.

Chen, J.J., Kipping, D., 2017. Probabilistic forecasting OF the masses and radii OF other worlds. Astrophys. J. 834.

Dahlen, F.A., Tromp, J., 1998. Theoretical Global Seismology. Princeton University Press, Princeton, New Jersey.

Darwin, G.H., 1898. The evolution of satellites. Atl. Mon. 81, 444–455.

Fuller, J., 2014. Saturn ring seismology: evidence for stable stratification in the deep interior of Saturn. Icarus 242, 283–296.

Fuller, J., Luan, J., Quataert, E., 2016. Resonance locking as the source of rapid tidal migration in the Jupiter and Saturn moon systems. Mon. Not. R. Astron. Soc. 458, 3867–3879.

Hesselbrock, A.J., Minton, D.A., 2017. An ongoing satellite–ring cycle of Mars and the origins of Phobos and Deimos. Nat. Geosci. 10, 266.

Holsapple, K.A., Michel, P., 2006. Tidal disruptions: a continuum theory for solid bodies. Icarus 183, 331–348.

Lognonné, P., Giardini, D., Banerdt, B., Gagnepain-Beyneix, J., Mocquet, A., Spohn, T., Karczewski, J., Schibler, P., Cacho, S., Pike, W., 2000. The NetLander very broad band seismometer. Planet. Space Sci. 48, 1289–1302.

Love, A.E.H., 1911. Some Problems of Geodynamics. University Press, Cambridge.

Marley, M.S., 1991. Nonradial oscillations of Saturn. Icarus 94, 420–435.

Marley, M.S., 2014. Saturn ring seismology: looking beyond first order resonances. Icarus 234, 194–199.

Marley, M.S., Porco, C.C., 1993. Planetary acoustic mode seismology: saturn's rings. Icarus 106, 508–524.

Murray, C.D., Dermott, S.F., 1999. Solar System Dynamics. Cambridge university press.

Nimmo, F., Faul, U.H., 2013. Dissipation at tidal and seismic frequencies in a melt-free, anhydrous Mars. J. Geo. Res. Planets 118, 2558–2569.

Nimmo, F., Spencer, J.R., Pappalardo, R.T., Mullen, M.E., 2007. Shear heating as the origin of the plumes and heat flux on Enceladus. Nature 447, 289–291.

Taylor, P.A., Margot, J.L., 2010. Tidal evolution of close binary asteroid systems. Celest. Mech. Dyn. Astron. 108, 315–338.

Zharkov, V., Gudkova, T., 1997. On the dissipative factor of the Martian interiors. Planet. Space Sci. 45, 401–407.

Zheng, Y., Malallah, A.H., Fehler, M.C., Hu, H., 2016. 2D full-waveform modeling of seismic waves in layered karstic media. Geophysics 81, T25–T34.

Zheng, Y., Nimmo, F., Lay, T., 2015. Seismological implications of a lithospheric low seismic velocity zone in Mars. Phys. Earth Planet. Inter. 240, 132–141.